NeuroImage xxx (xxxx) xxx–xxx

Contents lists available at ScienceDirect

NeuroImage

journal homepage: www.elsevier.com/locate/neuroimage

Relative latency and temporal variability of hemodynamic responses at the human primary visual cortex

Fa-Hsuan Lin[a,b], Jonathan R. Polimeni[c,d], Jo-Fu Lotus Lin[a], Kevin W.-K. Tsai[e], Ying-Hua Chu[a], Pu-Yeh Wu[a], Yi-Tien Li[a], Yi-Cheng Hsu[a], Shang-Yueh Tsai[f,g], Wen-Jui Kuo[h,*]

[a] *Institute of Biomedical Engineering, National Taiwan University, Taipei, Taiwan*
[b] *Department of Neuroscience and Biomedical Engineering, Aalto University, Espoo, Finland*
[c] *Athinoula A. Martinos Center for Biomedical Imaging, Department of Radiology, Harvard Medical School, Massachusetts General Hospital, Charlestown, MA 02129, USA*
[d] *Harvard-MIT Division of Health Sciences and Technology, Massachusetts Institute of Technology, Cambridge, MA, USA*
[e] *Aim for the Top University Project Office, National Taiwan Normal University, Taipei, Taiwan*
[f] *Institute of Applied Physics, National Chengchi University, Taipei, Taiwan*
[g] *Research Center for Mind Brain and Learning, National Chengchi University, Taipei, Taiwan*
[h] *Institute of Neuroscience, National Yang-Ming University, 155 Sec. 2, Li-Nung Street, Taipei 112, Taiwan*

ARTICLE INFO

Keywords:
fMRI
V1
Stability
Retinotopy
Precision
Hemodynamics

ABSTRACT

The blood-oxygen-level-dependent (BOLD) functional MRI (fMRI) signal is a robust surrogate for local neuronal activity. However, it has been shown to vary substantially across subjects, brain regions, and repetitive measurements. This variability represents a limit to the precision of the BOLD response and the ability to reliably discriminate brain hemodynamic responses elicited by external stimuli or behavior that are nearby in time. While the temporal variability of the BOLD signal at human visual cortex has been found in the range of a few hundreds of milliseconds, the spatial distributions of the average and standard deviation of this temporal variability have not been quantitatively characterized. Here we use fMRI measurements with a high sampling rate (10 Hz) to map the latency, intra- and inter-subject variability of the evoked BOLD signal in human primary (V1) visual cortices using an event-related fMRI paradigm. The latency relative to the average BOLD signal evoked by 30 stimuli was estimated to be 0.03 ± 0.20 s. Within V1, the absolute value of the relative BOLD latency was found correlated to intra- and inter-subject temporal variability. After comparing these measures to retinotopic maps, we found that locations with V1 areas sensitive to smaller eccentricity have later responses and smaller inter-subject variabilities. These correlations were found from data with either short inter-stimulus interval (ISI; average 4 s) or long ISI (average 30 s). Maps of the relative latency as well as inter-/intra-subject variability were found visually asymmetric between hemispheres. Our results suggest that the latency and variability of regional BOLD signal measured with high spatiotemporal resolution may be used to detect regional differences in hemodynamics to inform fMRI studies. However, the physiological origins of timing index distributions and their hemispheric asymmetry remain to be investigated.

Introduction

Regional functional magnetic resonance (fMRI) blood oxygenation level-dependent (BOLD) signals have been found stable across repetitive stimuli using linear system analysis (Boynton et al., 1996; Dale and Buckner, 1997). This temporal stability lays the foundation of using General Linear Model to localize functional brain areas. Characteristics of BOLD waveforms are found closely related to the time domain features of stimulation or behavioral responses: the inter-trial stimuli time in the range of seconds was correlated with the hemodynamic inter-peak timing at the human motor cortex (Kim et al., 1997). The latency difference between the BOLD signal at left and right motor cortices corresponded to the delay difference between the left and right hands motor responses separated by about 2 s (Miezin et al., 2000). Using a visuomotor task, the inter-regional timing between primary visual cortex (V1) and supplementary motor area (SMA) was significantly correlated to the reaction time in the ranges of hundreds of milliseconds (Menon et al., 1998). We also found that, across subjects, the order of inter-regional fMRI signals at visual and motor cortices with about 400 ms latency difference between them followed the order stimuli and behavior responses (Lin et al., 2013).

* Corresponding author.
E-mail address: wjkuo@ym.edu.tw (W.-J. Kuo).

http://dx.doi.org/10.1016/j.neuroimage.2017.01.041
Accepted 17 January 2017

While experimental evidence suggests that the BOLD signals are temporally stable, the variability of the BOLD signal has also been extensively reported. This variability was found different across regions, subjects, and measurement sessions. The variability of BOLD signal is directly related to the limit of detecting the correlation between hemodynamic and behavioral measurements (Aguirre et al., 1998; D'Esposito et al., 1999; Handwerker et al., 2004; Huettel and McCarthy, 2001). This variability also poses the limit of detecting information flows across brain regions using inter-regional hemodynamic measures. Quantitative information about the BOLD signal variability may be used to improve the power of detecting active brain areas using hierarchical analysis (Woolrich et al., 2004a, 2004b). The temporal bias and the instability of the fMRI signal may be modulated by attentional and other cognitive states. Fine temporal fMRI features may also be used to distinguish between healthy and diseases, as well as between stages of development and aging.

Local vasculature differences in the brain (Duvernoy et al., 1981) can underlie the variability of BOLD signals, because the BOLD signal is the surrogate hemodynamic measurements of task-related (Logothetis et al., 2001) and spontaneous (Laufs et al., 2003; Scholvinck et al., 2010) neuronal activity. The relationship between BOLD signal variability and vasculature is exemplified by the correlation between local vascular density and regional resting-state and task-related fMRI amplitudes (Vigneau-Roy et al., 2014). Even within the same functional area, BOLD response still varies considerably between subjects and within subjects. Across subjects and across locations at the human visual cortex, the variability of the time-to-peak (TTP) of the BOLD signal was found around 0.52 s (standard deviation) at human visual cortex; the intra-subject TTP variability was slightly larger (0.79 s) (de Zwart et al., 2005). However, the intra-subject variability of the BOLD signal was found smaller than the inter-subject variability at the human visual cortex in another study (Leontiev and Buxton, 2007) and at the human motor cortex (Aguirre et al., 1998). By further separating the intra-subject variability into the contribution across days and across sessions on the same day, it was found that the latter was more stable with a measured variability of a fraction of a second (Aguirre et al., 1998).

While the BOLD signal is mostly stable within-area, within-subject, and within-session, it still varies significantly across trials (Duann et al., 2002). Yet such within-session variability has not been systematically studied. Note that such variability across trials has been found correlated between neurophysiological measurements (P1 amplitudes from EEG) and hemodynamic measurements (time-to-peak in fMRI) (Bagshaw and Warbrick, 2007). Thus variation in neuronal activity, neurovascular coupling, and vascular response uncertainty can all account for this within-session variability. Furthermore, little is known about how the relative latency and the stability of the BOLD signal varies *within* and *across* functional areas along the hierarchy of the visual system.

The goal of this study is to map the hemodynamic timing characteristics in the human primary visual cortex (V1) using high temporal precision measurements. In particular, we aim at quantifying the average and the standard deviation of the relative latency of the BOLD signal between subjects. We also want to characterize the within-session temporal stability of the BOLD signal within individual subjects. These timing characteristics respectively denote the average and the standard deviation of the relative temporal shifts of the local hemodynamic response with respect to a local hemodynamic response template. Suggested by previous studies, this relative latency and timing variability may be in the range of a few hundreds of milliseconds (de Zwart et al., 2005; Leontiev and Buxton, 2007). These timing characteristics were further analyzed in V1 using probabilistic anatomical labels (Fischl et al., 2008; Hinds et al., 2008) and retinotopic map atlas (Benson et al., 2014, 2012).

We used simultaneous-multi-slice (SMS) inverse imaging (InI), a fast fMRI acquisition enabled by highly parallel detection, multi-slice encoding (Larkman et al., 2001), blipped controlled aliasing (CAIPI) EPI (Setsompop et al., 2012), simultaneous echo refocusing (SER) (Feinberg and Setsompop, 2013), and regularized reconstruction (Lin et al., 2006, 2008), to monitor the BOLD signals with 10 Hz sampling rate and 5 mm resolution. The local relatively latency can be related to temporal variability, presumably due to the relative venous contribution (de Zwart et al., 2005; Turner, 2002) and, potentially, reflect differences in response timing across the visual field, as central and peripheral representations have been shown to have different temporal properties (Maunsell et al., 1999). Further assuming a similar vasculature pattern relative to the cortical folding pattern across subjects, the spatial pattern of intra-subject variability may be similar to that of inter-subject variability distribution. Characterization of response variability are keys to quantifying the temporal precision of the hemodynamic response and can help provide an understanding of the potential temporal resolving power of the BOLD response.

Methods

Subjects and the task

Fourteen subjects (n = 14; age: 27 ± 6.6; 4 female) were recruited to this study with written informed consents approved by the Institute Review Board of National Taiwan University Hospital. In the experiment, visual stimuli extending to both left and right visual fields (8 Hz reversal rate; 500 ms duration) were presented to the subjects in a rapid event-related fMRI design. The checkerboard subtended about 16° visual angle (*i.e.*, out of 8° eccentricity) and was generated from twelve concentric rings of equal width. The stimuli were presented using PsychoPy (Peirce, 2007, 2008). The onset of each checkerboard reversal was randomized with a uniform distribution of inter-stimulus intervals (ISI) varying from 2 to 16 s (average 4 s). There were 60 stimulus trials in each run. Subjects were instructed to engage a motor task: subjects needed to press the button when the randomly presented letter at the center of the visual field matched to the target descried at the beginning of the imaging session. Four runs of data were collected. Each run lasted for four minutes.

Using rapid presentation of visual stimuli may raise the concern on the nonlinearity effect of the BOLD signal at the visual cortex (Birn and Bandettini, 2005; Birn et al., 2001; de Zwart et al., 2009; Huettel and McCarthy, 2000), even though previous studies show that the BOLD responses at the visual cortex are still linear with stimuli separated as short as 2 s (Dale and Buckner, 1997) and about 4 s (Liu et al., 2010). To address this concern, we performed another experiment (long-IsI experiment) with ISI = 30 s. Ten subjects (n = 10; age: 29 ± 5.4; 5 female) were recruited to this experiments. The checkerboard reversal visual stimuli were identical to those in the first experiment. Four runs of 4-min data, each of which had 8 stimulus trials, were collected from each subject.

MRI acquisition and reconstruction; regions-of-interest identification

All data were acquired from a 3T MRI scanner (Skyra, Siemens, Erlangen, Germany) using a 32-channel head coil array. Recently we developed simultaneous-multi-slice inverse imaging (SMS-InI) to acquire BOLD-contrast fMRI with a 10-Hz sampling rate (Chu et al., 2016). Specifically, SMS-InI collected 20 axial 4-mm thick slices with 1-mm gap between slices. These slices were separated into two slice groups, each of which had 10 slices and excited/read in 50 ms. Neighboring slices within each slice group were further separated by SER (Feinberg and Setsompop, 2013). Aliased slices were further separated by blipped CAIPI (Setsompop et al., 2012) by introducing 1/3 FOV shift in the phase-encoding (anterior-posterior) direction between neighboring aliased slices. Other imaging parameters were: flip angle = 30°, in-plane resolution = 5 mm × 5 mm, FOV = 210 × 210 × 210 mm^3, TR = 100 ms, and TE = 25/27.5 ms for two slice sets in SER. The flip angle choice was based on the Ernst' angle with

T_1 = 1 s and TR = 100 ms. To reconstruct volumetric images, we needed a 'reference scan', where partition encoding steps were added after slice group excitation. A reference scan was acquired before four runs of the accelerated scan, which used the same imaging parameters of a reference scan except that all partition encoding steps were discarded. Note that SMS-InI using a short TR (0.1 s) also included a T_1-weighted contrast: a higher image pixel value may be related to faster flow or reduced cerebral blood volume, which in turn can be related to vascular architecture/reactivity (for review, see (Gao and Liu, 2012)). Therefore, we also used the SMS-InI image intensity to crudely understand the physiological origin of these hemodynamic timing features.

Structural images for each subject were acquired using a 3D T_1-weighted pulse sequence (MP-RAGE: TR/TE/TI = 2530/3.3/1100 ms, flip angle = 7°, partition thickness = 1.33 mm, image matrix = 256 × 256, 192 partitions, field-of-view = 21 cm × 21 cm). The location of the gray-white matter boundary for each participant was estimated with an automatic segmentation algorithm to yield a triangulated mesh model with approximately 340,000 vertices (Dale et al., 1999; Fischl et al., 2001, 1999b). This cortical model was used to register individual's fMRI data to his/her own cortical surface space (Dale et al., 1999; Fischl et al., 1999b). Between-subject averaging was done by morphing individual data through a spherical coordinate system (Fischl et al., 1999a) implemented in FreeSurfer (https://surfer.nmr.mgh.harvard.edu).

The reconstruction of InI data was done by the regularized SENSE algorithm (Lin et al., 2005, 2004), which generated 2400 volumes of brain images for each run. We used the in vivo sensitivity method (Sodickson, 2000) to construct the imaging encoding matrix, because fMRI experiments are primarily concerned with relative changes of BOLD time series. In the *in vivo* sensitivity method (Sodickson, 2000), coil sensitivity maps were the reconstructed volumetric images without any shifting (along the phase encoding direction) and aliasing (along the slice direction) from the reference scan using data collected at each channel of the coil array. Potential noise in the time series related to spontaneous cardiac and respiratory cycles were suppressed by the DRIFTER algorithm (Sarkka et al., 2012), a Bayesian modeling method capable of dynamic tracking these fluctuations. We used General Linear Model (GLM) with finite impulse response (FIR) basis functions (30-s duration with 6-s pre-stimulus baseline) to estimate the hemodynamic responses elicited by the visual stimuli. These basis functions were chosen to avoid potential bias in estimating the shape of hemodynamic responses using a conventional parametric function (such as the canonical hemodynamic response function). Since our study focused at the primary visual cortex, the region-of-interest (ROI) was identified from the intersection of functional activity (the spatial distribution of the temporally average between 4 s and 7 s after visual stimulus onset with t statistics greater than 4.0; Bonferroni corrected p-value < 0.01) and anatomical atlas (FreeSurfer, version 5.1.0; http://surfer.nmr.mgh.harvard.edu).

Retinotopic maps were derived from the anatomical template of human striate and extrastriate cortex (Benson et al., 2014, 2012). The boundary of V1 was derived from the probabilistic labels provided by the FreeSurfer (Fischl et al., 2008; Hinds et al., 2008). Here we only analyzed the temporal characteristics of brain areas that fell into the intersection of anatomical and functional ROIs and within the range of our visual stimuli (i.e., eccentricity < 8°).

BOLD latency and variability estimation

The latency and the variability of the BOLD response at each cortical location were estimated from an ensemble of responses estimated by using a bootstrap approach. Specifically, a local template BOLD response at each ROI was first estimated for each subjects by averaging the hemodynamic response function estimated by General Linear Model using finite impulse response bases across all voxels within the defined ROI.

The ensemble of the BOLD responses for each participant was created by the following procedures: First, we arbitrarily separated all stimulus trials into two groups, each of which had 30 trials. Then hemodynamic responses were separately estimated for these two groups using GLM with FIR bases separately (see description above). Note that these estimates were the evoked fMRI signal across 30 trials, which may be temporally overlapped because of the arranged stimulus onsets and the duration (~20 s) of the hemodynamic response. However, using GLM allowed us to separate these overlapped responses. We repeated these two steps 30 times. This all together provided 60 bootstrap estimated BOLD responses across two groups.

Subsequently, we calculated the Pearson's correlation coefficient between the template BOLD response and each bootstrap estimate BOLD response from each bootstrap trial. Correlation coefficients were calculated with the template BOLD response temporally shifted forward and backward for ± 4 s at 0.1-s steps. The temporal shift that corresponded to the largest correlation coefficient was taken as the relative latency of a specific realization of the evoked BOLD response estimation.

All procedures described above were applied to each cortical location within each ROI in each participant. Thus we had 60 (bootstrap samples) × 14 (participants) = 840 response latency estimates at each cortical location in the atlas space. Accordingly, three metrics were calculated: 1) *Relative latency* was calculated as the average across all 840 response latency estimates. 2) *Intra-subject latency variability* was calculated by first taking the standard deviation across 60 bootstrap samples within each subject and then averaging across subjects. 3) *Inter-subject latency variability* was calculated by first averaging the relative latency across 60 bootstrap samples within each subject and then taking the standard deviation across subjects. All calculations were done using Matlab (Mathworks, Natick, MA, USA).

Results

Our stimuli elicited strong BOLD signal at the visual cortices at both hemispheres. Fig. 1 top panel shows the spatial distribution of average (4 s and 7 s post the onset of the visual stimulus) t-statistics maps and time courses within V1 of the left and right hemispheres from experiments with average ISI = 4 s and average ISI = 30 s. We noticed that the amplitude of BOLD signal showed a gradient in the anterior-posterior direction. However, areas with low t-statistics were mostly outside the 8° eccentricity. Thus we considered that the chosen ROI had the minimal impact on the sensitivity for resolving regional differences in latency. The V1 regions-of-interest in this study were shown in the middle panel of Fig. 1. The bottom panel of Fig. 1 shows the retinotopic maps of the eccentricity and polar angles at the left hemisphere. They were subsequently used to correlate to the BOLD relative latency, intra-subject variability and inter-subject variability.

Histograms of the relative latency at V1 were shown in Fig. 2. The distribution at V1 was normally distributed (Chi-square test; Chi-square = 5.00; p = 0.42). Across locations in V1, the average and the standard deviation of the relative latency were 0.03 s and 0.20 s (intra-subject variability)/0.35 s (inter-subject variability), respectively. The range of intra-subject variability was smaller (0.7 s) than that of inter-subject variability (1.0 s). The average and the standard deviation of the intra-subject latency variability were 0.20 s and 0.14 s, respectively. The inter-subject latency variability at V1 was 0.35 ± 0.21 s. Distributions of relative latency and both variability measures are shown in Fig. 2.

Spatial distributions of the relative latency, intra-subject latency variability, and inter-subject latency variability from data with average ISI of 4 s are shown in Fig. 3. Brain locations closer to the fundus of the calcalrine sulcus showed earlier BOLD response (more negative relative latency). The intra-subject latency variability at V1 was mostly under 1 s. Smaller intra- and inter-subject variability was observed around the fundus of the calcarine sulcus. The relative latency and maps were visually different between hemispheres. However, the areas showing

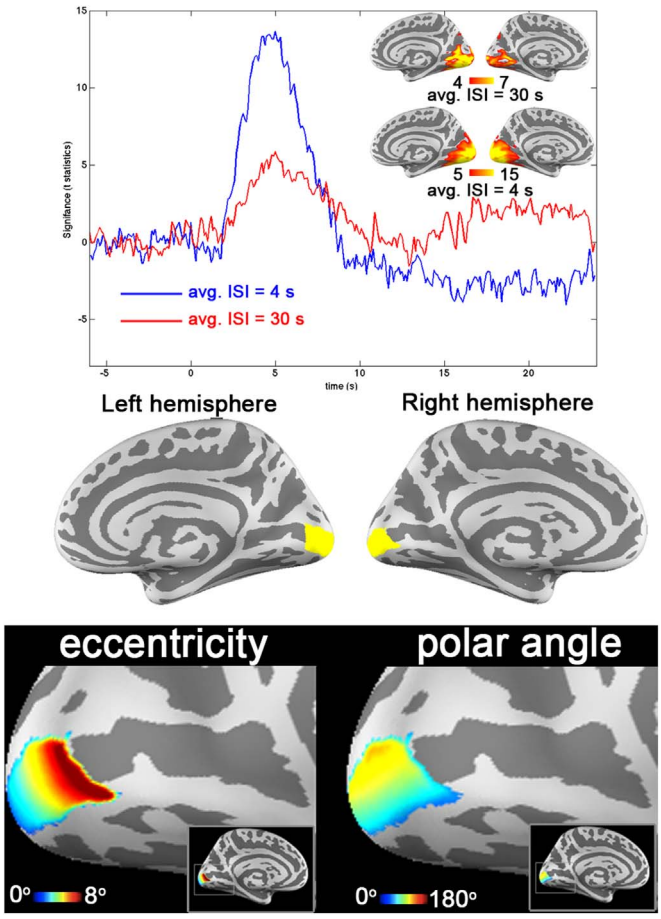

Fig. 1. Top: average time courses between left and right visual cortices using short ISI (4 s) and long ISI (30 s) data. Visual cortices were defined as the average of the dynamic *t*-statistics maps between 4 s and 7 s after visual stimulus onset. The spatial distributions of average t-statistics were shown in the inlet. Middle: Primary visual cortex regions-of-interest (yellow) on inflated cortical surfaces. Bottom: Retinotopic maps of eccentricity within 8 degrees and polar angle at V1 of the left hemisphere based on an atlas. (For interpretation of the references to color in this figure legend, the reader is referred to the web version of this article).

larger relative latency had also larger variability (about one standard deviation; bottom row of Fig. 3), suggesting that the difference between hemispheres may not be significant. Note that our maps also show anterior-posterior gradients and inferior-to-superior differences, which may be also related to vasculature. Taken together, the origin of inter-hemispheric asymmetry and intra-hemispheric distributions is not yet fully understood here and requires additional studies in a larger number of subjects and vascular anatomy as well as reactivity mapping.

Fig. 4 shows spatial distributions of the relative latency, intra-subject latency variability, and inter-subject latency variability from

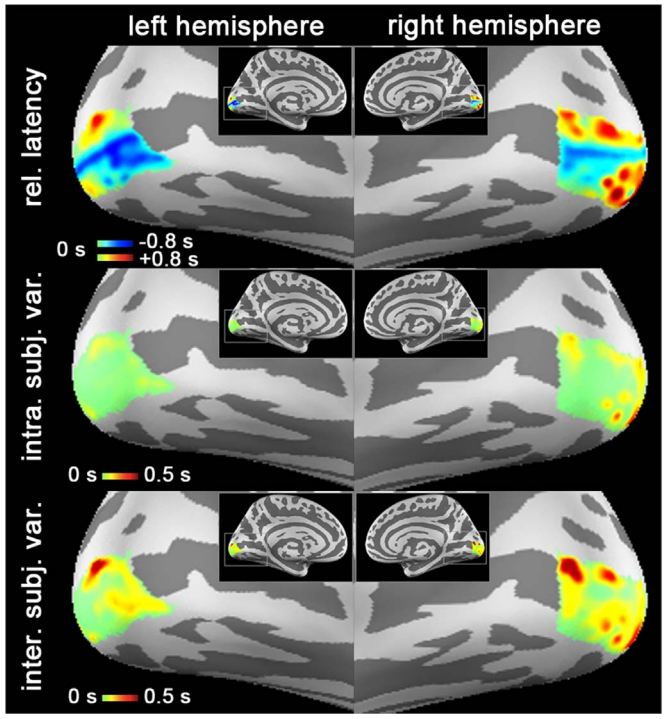

Fig. 3. Distributions of the relative latency (top), intra-subject latency variability (middle), inter-subject latency variability (bottom) at left and right hemispheres in the average 4-s ISI experiment.

data with average ISI of 30 s. They were visually similar to Fig. 3. However, the noise level became higher, potentially because of the smaller number of trials (32 trials) in the long ISI experiment compared with the short ISI experiment (240 trials).

The absolute value of relative latency, intra-subject latency variability, and inter-subject latency variability were correlated between each other at V1 (Fig. 5). The correlations between the intra-/inter-subject variability and the absolute value of the relative latency were significant ($p < 0.001$). We also found that, within V1, locations with a larger intra-subject latency variability were found to have with a larger inter-subject variability (slope = 1.10; $t = 11.55$; $p < 0.001$).

We attempted to further understand the correlation between relative latency and inter-/intra-subject in a physiologically meaningful coordinate system. Thus we correlated between BOLD timing characteristics and retinotopic maps. Considering the cortical magnification, we further analyzed the correlation between BOLD timing characteristics and the logarithm of the eccentricity. Results show that the logarithm of the eccentricity was negatively correlated with the relative latency (slope = 17.8 ms/log(degree); $t = -4.58$; $p < 0.001$) and positively correlated with inter-subject variability (slope = 12.4 ms/log(degree); $t = 2.52$; $p < 0.001$). The top row in Fig. 6 shows the plots

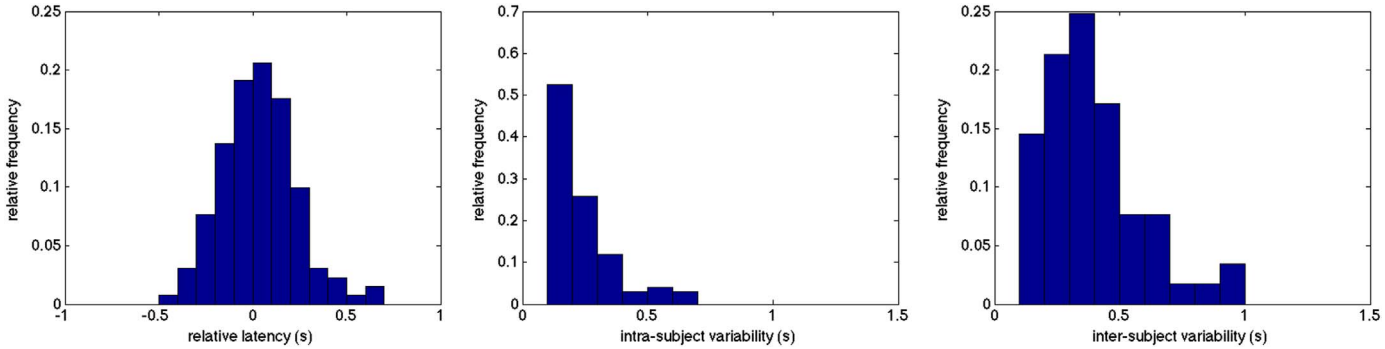

Fig. 2. Distributions of the relative latency of V1 (left), intra-subject latency variability (middle), and inter-subject latency variability (right) across the V1 ROI.

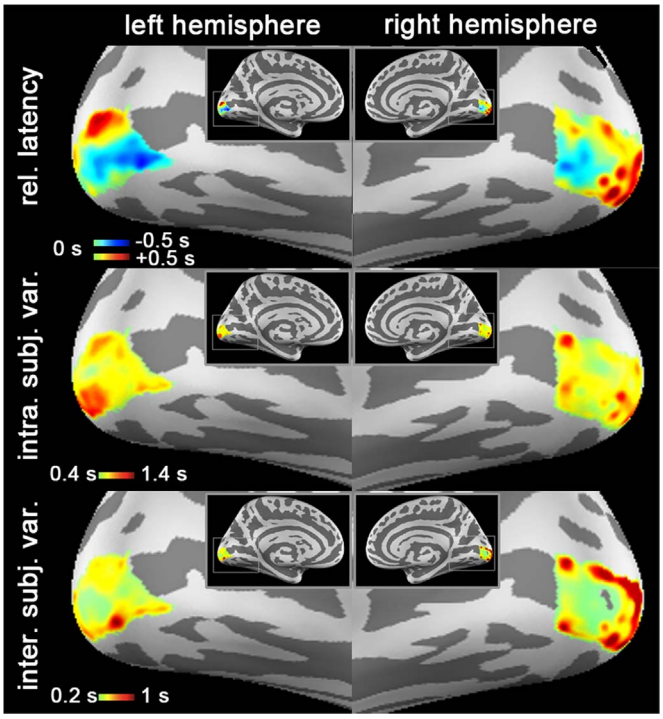

Fig. 4. Distributions of the relative latency (top), intra-subject latency variability (middle), inter-subject latency variability (bottom) at left and right hemispheres in the average 30-s ISI experiment.

comparing latency with the logarithm of the eccentricity of the visual field representation. Using the long ISI data, we found similar correlations (the bottom row in Fig. 6): 1) the relative latency is shorter at areas more sensitive to peripheral vision, 2) the inter-subject variability at areas sensitive to peripheral vision is larger than at areas sensitive to foveal vision, and 3) the intra-subject variability is not significantly correlated with the visual eccentricity.

No significant correlation was found between the polar angle distribution and relative latency, intra-subject, or inter-subject variability at V1. However, as we correlated to the polar angle distance to the horizontal meridian and timing characteristics, we found that inter-subject variability is significantly correlated with this polar angle distance using average ISI = 4 s data. The same correlation was also found using average ISI = 30 s data, which also suggested significant correlation to the relative latency (Fig. 7). Specifically, inter-subject variability is higher at locations further away from the horizontal meridian (~4 to 6 ms/degree increase). We also found that, using ISI = 30 s data, the relative latency and the distance from the horizontal meridian was significantly correlated. These correlations may be related to the underlying vascular structure or vascular reactivity. Additional specific measurements are needed to clarify this possibility.

Discussion

In this study, we systematically delineated and quantified the average and the standard deviation of the relative latency of visual cortex hemodynamics using high temporal precision fMRI data. The range of the relative latency in the visual cortex was about 1 s at V1 (Fig. 2). The observed variability is in agreement with early studies (de Zwart et al., 2005; Lee et al., 1995). Previous studies suggested that the BOLD signals progressively becomes more stable as the measurements are taken closer in time, *i.e.*, between days and within a day, (Aguirre et al., 1998). Our results show that, even within the same measurement session on the same day, the BOLD signals still vary significantly across trials. Specifically, for the evoked response estimated from 30 stimulus trials randomly distributed over 4 min, it has about 0.3 s temporal instability. This intra-subject variability distribution was closely related to the inter-subject variability distribution (Figs. 3–5). The relationship between the relative latency and the intra-/inter-subject variability is rather complex: relative latency and the absolute value of relative latency both correlated to intra- and inter-subject variability (Fig. 5). This association was further elucidated with the help of retinotopic maps (Figs. 6 and 7): in the primary visual cortex, posterior locations near the central-field representation have later responses (lager relative latency) and anterior locations near the peripheral field representation have lower stability (larger inter-subject variability). The inter-subject variability was also found significantly correlated to the polar angle distance to the horizontal meridian (Fig. 7). Because the major supplying arteries and draining veins of the calcarine sulcus tend to be oriented in the anterior-posterior direction (Duvernoy et al., 1981), there may be features of the macrovascular anatomy that impart some of the observed systematic relationship between the variance in the BOLD responses to visual stimulation and the eccentricity axis of the retinotopic representation. The finding that the inter-subject variability, but not intra-subject variability, is significantly correlated to eccentricity (Fig. 6) and polar angle distance to the horizontal meridian (Fig. 7), may also be attributed to variable venous structure or reactivity across subjects.

To partially test our hypothesis on the venous contribution to the BOLD timing characteristics studied here, we correlated between the relative latency and intra-/inter-subject variability and SMS-InI image intensity, which is physiologically related to in-flow effects, cerebral flood volume, and BOLD contrast. We found that both the relative latency and the intra-subject variability were significantly correlated with the image pixel value (Fig. 8). While this analysis partially

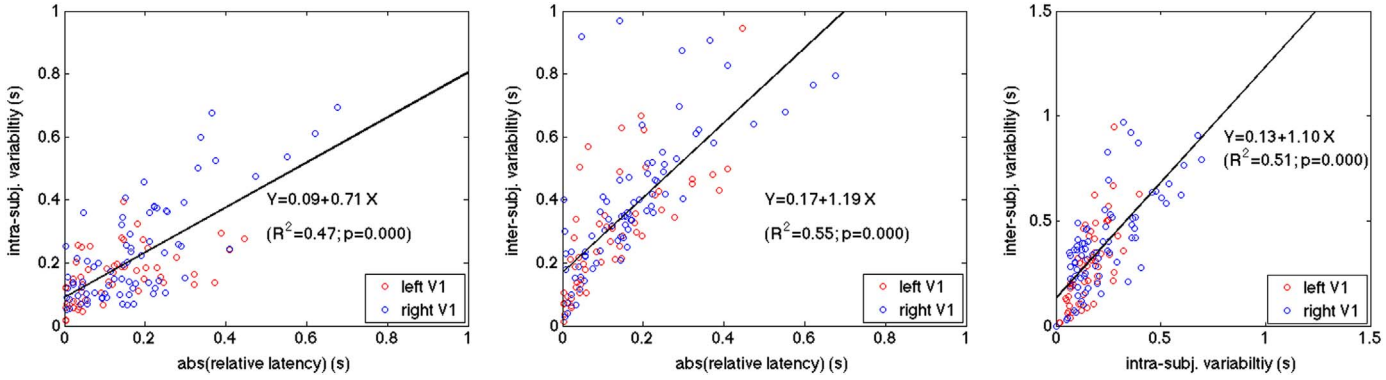

Fig. 5. Correlations between the absolute value of the relative latency and intra-subject latency variability (left) as well as between the absolute value of the relative latency and inter-subject variability (middle). These two correlations were found significant. Right: the significant correlation between intra-subject and inter-subject latency variability. All plots were based on data collected across ROIs in the left and right V1. The significance of the correlation was quantified by R^2 and *p*-value, which were both reported in the figure.

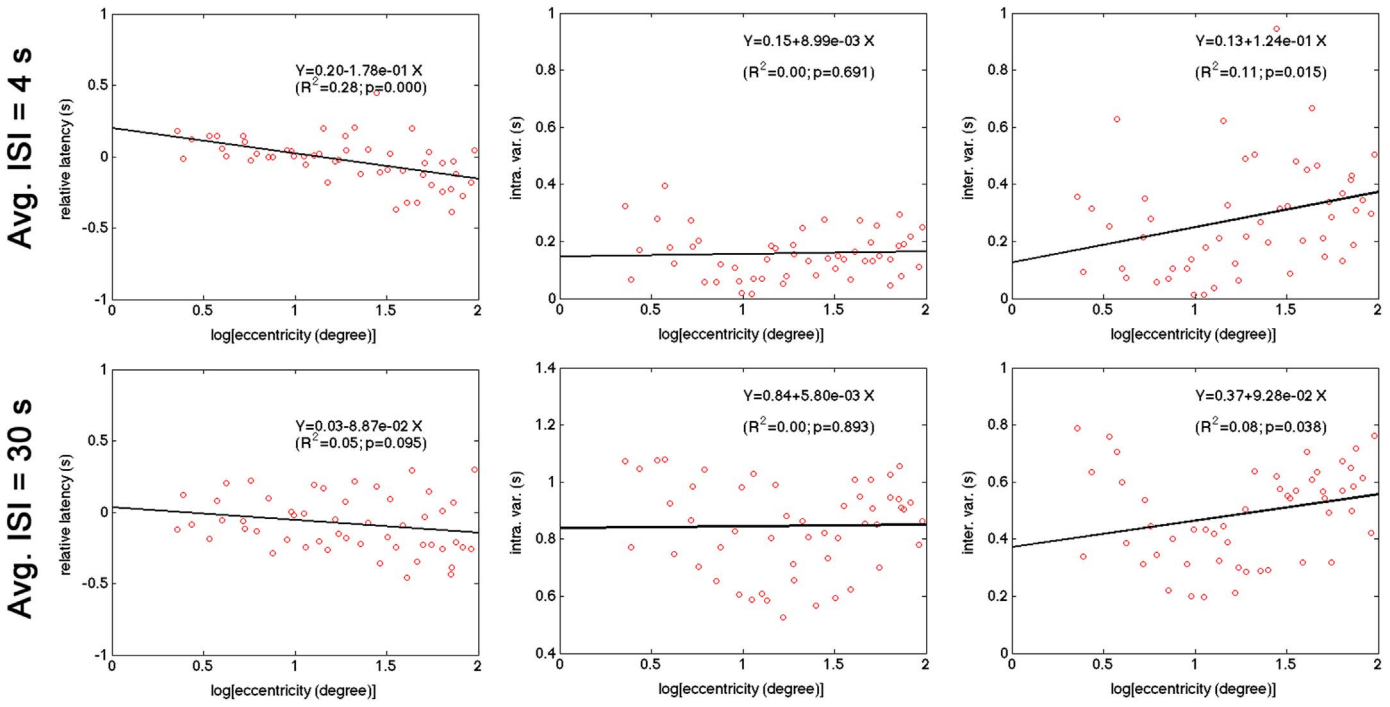

Fig. 6. Correlation between relative latency (left), intra-subject variability (middle), and inter-subject variability (right) across ROIs in V1 to the logarithm of the eccentricity using data with average ISI=4 s (top row) and average ISI=30 s (bottom row). Relative latency and inter-subject variability were both significantly correlated to eccentricity.

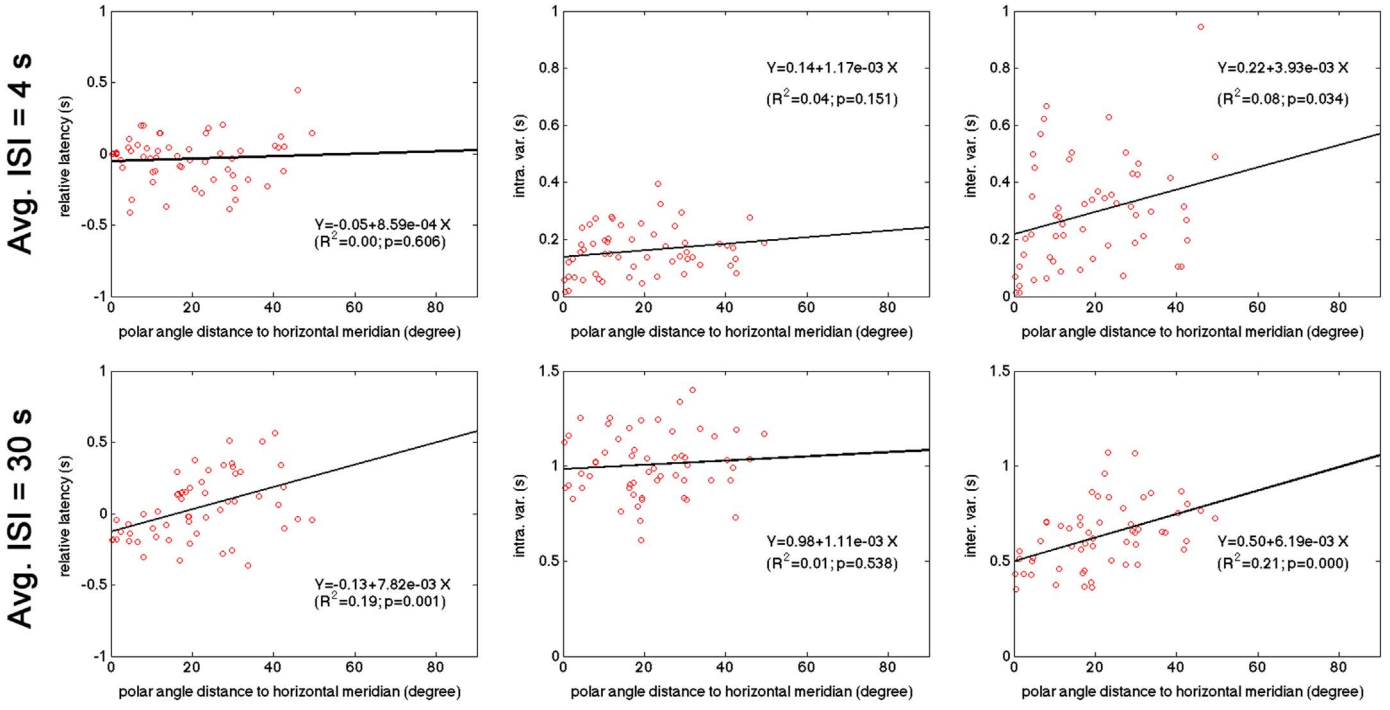

Fig. 7. Correlation between relative latency (left), intra-subject variability (middle), and inter-subject variability (right) across ROIs in V1 to the polar angle distance to the horizontal meridian using data with average ISI=4 s (top row) and average ISI=30 s (bottom row). Relative latency and inter-subject variability were both significantly correlated to eccentricity.

supported our hypothesis, we believe that more sensitive and direct measurements of venous structure, such as vascular density mapping based on susceptibility-weighted imaging (Vigneau-Roy et al., 2014), and vascular reactivity, such as using a breath-holding task (Chang et al., 2008), may clarify the physiological origins of these timing features more accurately. This will be explored in the near future.

Previously the correlation between the BOLD signal width (quantified by the full-width-half-maximum) and its time-to-peak has been demonstrated (de Zwart et al., 2005). It was inferred that brain areas with later time-to-peak and wider width in the BOLD signal are more closely related to venous contribution. The significant correlation between the relative latency and the intra-/inter-subject variability (Fig. 4) provided further empirical evidences that brain regions with relative later responses may be closely related to more venous contributions, which in turn caused larger variability in the response. Brain areas with more venous contribution have three timing characteristics in its local hemodynamic response: longer latency, wider BOLD signal peak, and larger timing variability.

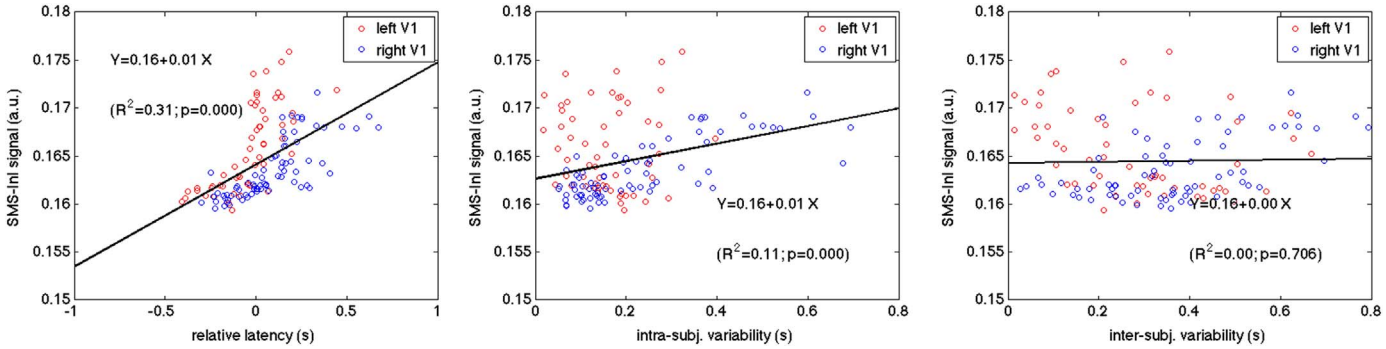

Fig. 8. Correlation between the image intensity and the relative latency (left), intra-subject variability (middle), as well as inter-subject variability (right) at V1. Relative latency and intra-subject variability were significantly correlated to the image intensity of SMS-InI data.

In addition to attributing relative latency and BOLD signal stability to vascular contribution, it is also possible that these timing characteristics can be related to neuronal activity. However, this speculation cannot be confirmed by our results, because we did not control local vascular reactivity. Further experiments using measurements directly sensitive to neuronal activity, such as EEG and MEG, may provide necessary information.

The variability found here was smaller than the variability reported in an earlier study: intra-subject variability was about 1.2 ± 2.1 s (Saad et al., 2001). The difference may be due to that we specifically examined the variability at V1 and V2, while the previous study (Saad et al., 2001) examined the whole visual cortex. The difference in the stimuli presentation (block design by Saad et al. *vs*. event-related design in this study) and the data sampling method (2 s sampling rate by Saad et al. and 0.1 s sampling rate in this study) may also be a reason.

We want to clarify that the timing variability described in this study was not the temporal uncertainty of single-trial responses. Note that, in order to resolve the issues of low SNR in typical fMRI experiments and overlapped hemodynamic responses elicited across randomized trials with short inter-stimulus intervals, we developed a bootstrap approach to estimate the variability of the evoked response elicited from 30 trials. This uncertainty can become smaller for the evoked response elicited from more trials or more subjects. Our results provided quantitative information about the 'temporal effective size' in fMRI experiments to facilitate the estimation of necessary stimulus trials, averages, and subjects. Furthermore, these variability estimates can be applied to hierarchical modeling of the fMRI analysis (Woolrich et al., 2004a, 2004b).

The choice of the 30° flip angle in this study was based on the calculation of the Ernst' angle with TR = 0.1 s and T_1 of 1 s. It has been reported that T_2^*-weighted fMRI signal has contributions from both in-flow effects and BOLD contrast. The in-flow effects are more prominent with stronger T_1-weighting using a short TR and a large flip angle (Gao and Liu, 2012). In the future, we may further improve the functional specificity of our measurements by using a smaller flip angle.

Our results signify the advantage of measuring the BOLD signal with high temporal precision. The regression analyses were enabled by the data distributed over one second (Fig. 5). Thus our sub-second sampling indeed delineated hemodynamic response features that have been ignored by acquisitions with a sampling rate slower than 1 Hz. Note that our method also has sufficient spatial resolution to discern responses at different locations in V1. While not directly demonstrated in this study, our measurements on the variability of BOLD signal can be important in understanding the limit of detecting the correlation between hemodynamic and behavioral measurements (Aguirre et al., 1998; D'Esposito et al., 1999; Handwerker et al., 2004; Huettel and McCarthy, 2001). Specifically, such correlations between behaviors and inter-/intra-regional evoked hemodynamic responses should consider local temporal dispersion reported in this study in order avoid the bias of attributing local vascular reactivity variance to neuronal activity variance. The temporal bias and the instability of the fMRI signal reported here may be different between cognitive states (such as attentional level), diseases, and development/aging. Further studies are necessary to test this speculation. The physiological origins of timing index distributions and their hemispheric asymmetry reported here also remain to be investigated.

Limitations of our study include the use of relatively simple and artificial stimuli to generate functional activity at the visual cortex. Different temporal characteristic of the BOLD signal may be derived from experiments using different stimuli, *e.g*., naturalistic faces and landscapes. Different functional areas and population groups may also demonstrate distinct features. Encouraged by the acquisition/analysis method and results reported here, we are optimistic in exploring the correlation between fine temporal features in the hemodynamic responses measured by high precision measurements and brain function.

Acknowledgement

Authors thank Drs. Geoffrey Aguirre and Andrew Bock for their help with the retinotopic atlas. This work was partially supported by Ministry of Science and Technology, Taiwan (103-2628-B-002-002-MY3, 104-2410-H-010 -003 -MY2, 105-2221-E-002-104), the Academy of Finland (No. 298131), and NIH National Institute for Biomedical Imaging and Bioengineering (P41-EB015896 and R01-EB019437).

References

Aguirre, G.K., Zarahn, E., D'Esposito, M., 1998. The variability of human, BOLD hemodynamic responses. Neuroimage 8, 360–369.
Bagshaw, A.P., Warbrick, T., 2007. Single trial variability of EEG and fMRI responses to visual stimuli. Neuroimage 38, 280–292.
Benson, N.C., Butt, O.H., Brainard, D.H., Aguirre, G.K., 2014. Correction of distortion in flattened representations of the cortical surface allows prediction of V1-V3 functional organization from anatomy. PLoS Comput. Biol. 10, e1003538.
Benson, N.C., Butt, O.H., Datta, R., Radoeva, P.D., Brainard, D.H., Aguirre, G.K., 2012. The retinotopic organization of striate cortex is well predicted by surface topology. Curr. Biol. 22, 2081–2085.
Birn, R.M., Bandettini, P.A., 2005. The effect of stimulus duty cycle and "off" duration on BOLD response linearity. Neuroimage 27, 70–82.
Birn, R.M., Saad, Z.S., Bandettini, P.A., 2001. Spatial heterogeneity of the nonlinear dynamics in the FMRI BOLD response. Neuroimage 14, 817–826.
Boynton, G.M., Engel, S.A., Glover, G.H., Heeger, D.J., 1996. Linear systems analysis of functional magnetic resonance imaging in human V1. J. Neurosci. 16, 4207–4221.
Chang, C., Thomason, M.E., Glover, G.H., 2008. Mapping and correction of vascular hemodynamic latency in the BOLD signal. Neuroimage 43, 90–102.
Chu, Y.H., Hsu, Y.C., Lin, F.H., 2016. Simultaneous multi-slice inverse imaging for high temporal resolution fMRI. Proc. Int. Soc. Magn. Reson. Med., 946.
D'Esposito, M., Zarahn, E., Aguirre, G.K., Rypma, B., 1999. The effect of normal aging on the coupling of neural activity to the bold hemodynamic response. Neuroimage 10, 6–14.
Dale, A.M., Buckner, R.L., 1997. Selective averaging of rapidly presented individual trials using fMRI. Hum. Brain Mapp. 5, 329–340.
Dale, A.M., Fischl, B., Sereno, M.I., 1999. Cortical surface-based analysis. I. Segmentation and surface reconstruction. Neuroimage 9, 179–194.

de Zwart, J.A., Silva, A.C., van Gelderen, P., Kellman, P., Fukunaga, M., Chu, R., Koretsky, A.P., Frank, J.A., Duyn, J.H., 2005. Temporal dynamics of the BOLD fMRI impulse response. Neuroimage 24, 667–677.
de Zwart, J.A., van Gelderen, P., Jansma, J.M., Fukunaga, M., Bianciardi, M., Duyn, J.H., 2009. Hemodynamic nonlinearities affect BOLD fMRI response timing and amplitude. Neuroimage 47, 1649–1658.
Duann, J.R., Jung, T.P., Kuo, W.J., Yeh, T.C., Makeig, S., Hsieh, J.C., Sejnowski, T.J., 2002. Single-trial variability in event-related BOLD signals. Neuroimage 15, 823–835.
Duvernoy, H.M., Delon, S., Vannson, J.L., 1981. Cortical blood vessels of the human brain. Brain Res. Bull. 7, 519–579.
Feinberg, D.A., Setsompop, K., 2013. Ultra-fast MRI of the human brain with simultaneous multi-slice imaging. J. Magn. Reson. 229, 90–100.
Fischl, B., Liu, A., Dale, A.M., 2001. Automated manifold surgery: constructing geometrically accurate and topologically correct models of the human cerebral cortex. IEEE Trans. Med. Imaging 20, 70–80.
Fischl, B., Rajendran, N., Busa, E., Augustinack, J., Hinds, O., Yeo, B.T., Mohlberg, H., Amunts, K., Zilles, K., 2008. Cortical folding patterns and predicting cytoarchitecture. Cereb. Cortex 18, 1973–1980.
Fischl, B., Sereno, M., Tootell, R., Dale, A., 1999a. High-resolution inter-subject averaging and a coordinate system for the cortical surface. Hum. Brain Mapp. 8, 272–284.
Fischl, B., Sereno, M.I., Dale, A.M., 1999b. Cortical surface-based analysis. I. Segmentation and surface reconstruction. Neuroimage 9, 195–207.
Gao, J.H., Liu, H.L., 2012. Inflow effects on functional MRI. Neuroimage 62, 1035–1039.
Handwerker, D.A., Ollinger, J.M., D'Esposito, M., 2004. Variation of BOLD hemodynamic responses across subjects and brain regions and their effects on statistical analyses. Neuroimage 21, 1639–1651.
Hinds, O.P., Rajendran, N., Polimeni, J.R., Augustinack, J.C., Wiggins, G., Wald, L.L., Diana Rosas, H., Potthast, A., Schwartz, E.L., Fischl, B., 2008. Accurate prediction of V1 location from cortical folds in a surface coordinate system. Neuroimage 39, 1585–1599.
Huettel, S.A., McCarthy, G., 2000. Evidence for a refractory period in the hemodynamic response to visual stimuli as measured by MRI. Neuroimage 11, 547–553.
Huettel, S.A., McCarthy, G., 2001. The effects of single-trial averaging upon the spatial extent of fMRI activation. Neuroreport 12, 2411–2416.
Kim, S.G., Richter, W., Ugurbil, K., 1997. Limitations of temporal resolution in functional MRI. Magn. Reson. Med. 37, 631–636.
Larkman, D.J., Hajnal, J.V., Herlihy, A.H., Coutts, G.A., Young, I.R., Ehnholm, G., 2001. Use of multicoil arrays for separation of signal from multiple slices simultaneously excited. J. Magn. Reson. Imaging 13, 313–317.
Laufs, H., Krakow, K., Sterzer, P., Eger, E., Beyerle, A., Salek-Haddadi, A., Kleinschmidt, A., 2003. Electroencephalographic signatures of attentional and cognitive default modes in spontaneous brain activity fluctuations at rest. Proc. Natl. Acad. Sci. USA 100, 11053–11058.
Lee, A.T., Glover, G.H., Meyer, C.H., 1995. Discrimination of large venous vessels in time-course spiral blood-oxygen-level-dependent magnetic-resonance functional neuroimaging. Magn. Reson. Med. 33, 745–754.
Leontiev, O., Buxton, R.B., 2007. Reproducibility of BOLD, perfusion, and CMRO2 measurements with calibrated-BOLD fMRI. Neuroimage 35, 175–184.
Lin, F.H., Huang, T.Y., Chen, N.K., Wang, F.N., Stufflebeam, S.M., Belliveau, J.W., Wald, L.L., Kwong, K.K., 2005. Functional MRI using regularized parallel imaging acquisition. Magn. Reson. Med. 54, 343–353.
Lin, F.H., Kwong, K.K., Belliveau, J.W., Wald, L.L., 2004. Parallel imaging reconstruction using automatic regularization. Magn. Reson. Med. 51, 559–567.
Lin, F.H., Wald, L.L., Ahlfors, S.P., Hamalainen, M.S., Kwong, K.K., Belliveau, J.W., 2006. Dynamic magnetic resonance inverse imaging of human brain function. Magn. Reson. Med. 56, 787–802.
Lin, F.H., Witzel, T., Mandeville, J.B., Polimeni, J.R., Zeffiro, T.A., Greve, D.N., Wiggins, G., Wald, L.L., Belliveau, J.W., 2008. Event-related single-shot volumetric functional magnetic resonance inverse imaging of visual processing. Neuroimage 42, 230–247.
Lin, F.H., Witzel, T., Raij, T., Ahveninen, J., Tsai, K.W., Chu, Y.H., Chang, W.T., Nummenmaa, A., Polimeni, J.R., Kuo, W.J., Hsieh, J.C., Rosen, B.R., Belliveau, J.W., 2013. fMRI hemodynamics accurately reflects neuronal timing in the human brain measured by MEG. Neuroimage 78, 372–384.
Liu, Z., Rios, C., Zhang, N., Yang, L., Chen, W., He, B., 2010. Linear and nonlinear relationships between visual stimuli, EEG and BOLD fMRI signals. Neuroimage 50, 1054–1066.
Logothetis, N.K., Pauls, J., Augath, M., Trinath, T., Oeltermann, A., 2001. Neurophysiological investigation of the basis of the fMRI signal. Nature 412, 150–157.
Maunsell, J.H., Ghose, G.M., Assad, J.A., McAdams, C.J., Boudreau, C.E., Noerager, B.D., 1999. Visual response latencies of magnocellular and parvocellular LGN neurons in macaque monkeys. Vis. Neurosci. 16, 1–14.
Menon, R.S., Luknowsky, D.C., Gati, J.S., 1998. Mental chronometry using latency-resolved functional MRI. Proc. Natl. Acad. Sci. USA 95, 10902–10907.
Miezin, F.M., Maccotta, L., Ollinger, J.M., Petersen, S.E., Buckner, R.L., 2000. Characterizing the hemodynamic response: effects of presentation rate, sampling procedure, and the possibility of ordering brain activity based on relative timing. Neuroimage 11, 735–759.
Peirce, J.W., 2007. PsychoPy–Psychophysics software in Python. J. Neurosci. Methods 162, 8–13.
Peirce, J.W., 2008. Generating stimuli for neuroscience using PsychoPy. Front. Neuroinform. 2, 10.
Saad, Z.S., Ropella, K.M., Cox, R.W., DeYoe, E.A., 2001. Analysis and use of FMRI response delays. Hum. Brain Mapp. 13, 74–93.
Sarkka, S., Solin, A., Nummenmaa, A., Vehtari, A., Auranen, T., Vanni, S., Lin, F.H., 2012. Dynamic retrospective filtering of physiological noise in BOLD fMRI: drifter. Neuroimage 60, 1517–1527.
Scholvinck, M.L., Maier, A., Ye, F.Q., Duyn, J.H., Leopold, D.A., 2010. Neural basis of global resting-state fMRI activity. Proc. Natl. Acad. Sci. USA 107, 10238–10243.
Setsompop, K., Gagoski, B.A., Polimeni, J.R., Witzel, T., Wedeen, V.J., Wald, L.L., 2012. Blipped-controlled aliasing in parallel imaging for simultaneous multislice echo planar imaging with reduced g-factor penalty. Magn. Reson. Med. 67, 1210–1224.
Sodickson, D.K., 2000. Tailored SMASH image reconstructions for robust in vivo parallel MR imaging. Magn. Reson Med. 44, 243–251.
Turner, R., 2002. How much cortex can a vein drain? Downstream dilution of activation-related cerebral blood oxygenation changes. Neuroimage 16, 1062–1067.
Vigneau-Roy, N., Bernier, M., Descoteaux, M., Whittingstall, K., 2014. Regional variations in vascular density correlate with resting-state and task-evoked blood oxygen level-dependent signal amplitude. Hum. Brain Mapp. 35, 1906–1920.
Woolrich, M.W., Behrens, T.E., Smith, S.M., 2004a. Constrained linear basis sets for HRF modelling using Variational Bayes. Neuroimage 21, 1748–1761.
Woolrich, M.W., Jenkinson, M., Brady, J.M., Smith, S.M., 2004b. Fully Bayesian spatio-temporal modeling of FMRI data. IEEE Trans. Med. Imaging 23, 213–231.